Polymer 51 (2010) 2585–2596

Contents lists available at ScienceDirect

Polymer

journal homepage: www.elsevier.com/locate/polymer

The effects of molecular weight and polymorphism on the fracture and thermo-mechanical properties of a carbon-fibre composite modified by electrospun poly (vinylidene fluoride) membranes

K. Magniez [a,b,*], C. De Lavigne [a,b], B.L. Fox [a]

[a] Institute for Technology Research and Innovation, Deakin University, Waurn Ponds, Victoria 3217, Australia
[b] École nationale supérieure des arts et industries textiles (ENSAIT), Roubaix 59056, France

ARTICLE INFO

Article history:
Received 21 January 2010
Received in revised form
30 March 2010
Accepted 9 April 2010
Available online 18 April 2010

Keywords:
Polyvinylidene fluoride
Electrospinning
Composites

ABSTRACT

The interlaminar toughening of a carbon-fibre reinforced composite by incorporation of electrospun polyvinylidene fluoride (PVDF) nanofibrous membranes was explored in this work. The electrospinning process of low and high molecular weight PVDF was optimised to form nanofibres free of defects with diameters averaging several hundred nanometres. The nanofibres were electrospun directly onto commercial pre-impregnated carbon fibre materials and under these optimised conditions, PVDF primarily crystallised in its β phase polymorphic form but significant variations were observed between samples. There is strong evidence from DMTA analysis to suggest that a partial miscibility between the amorphous phases of the PVDF nanofibres and the epoxy exists. The improved plastic deformation at the crack tip after inclusion of the nanofibres was directly translated to a 57% increase in the mode II interlaminar fracture toughness (in-plane shear failure). Conversely, the fracture toughness in mode I (opening failure) was slightly lower than the reference by approximately 20%, and the results were interpreted from the complex micromechanisms of failure arising from the changes in polymorphism and molecular weight of the PVDF.

1. Introduction

Owing to their exceptional engineering properties, carbon fibre reinforced composites belong to a class of advanced material which have witnessed significant progress in recent years. More recently, these materials have rapidly become a material of choice as alternative replacement to other traditional materials and have found applications in the automotive and aerospace sectors. The new Boeing 787 is modern example of technological achievement that utilise up to 50 weight percent of lightweight composite materials [1]. Nonetheless, the inherent brittleness of epoxy resins has restricted their implementation into structural components requiring certain levels of toughness. For the past decade, the improvement in the fracture toughness of composite materials has been the centre of attention amongst the scientific and industrial communities [2,3]. This has been realised through the development of novel resin systems involving the use of rubbers and thermoplastics as toughening agents [2,4]. Interlayer toughening described as the inclusion of discrete layers of a secondary material, in film, fibrous or particulate form, in the inter-plies region has also been successfully applied [3,5–10].

Very recently, the interlayer toughening of carbon fibre reinforced composites using a nanofibrous substrate produced by electrospinning has been reported but thus far this approach remains novel as very limited literature has been published [11–15]. The pioneering concept patented by Dzenis [11] was successfully applied by Li et al. who reported significant enhancements in the resistance to delamination (mode I) of a carbon fibre reinforced composites using polysulfone (PSF) nanofibres [12,13]. Others only reported more modest variations using polybenzimidazole (PBI) [11] and epoxy [14] nanofibres. Sihn et al. found that the number of microcracks generated from delamination stresses during uniaxial tension loading decreased by nearly 22% after incorporation of electrospun polycarbonate nanofibres (200 nm average diameter) in the inter-ply regions [15].

Polyvinylidene fluoride (PVDF) is a well-known thermoplastic that possess excellent engineering properties such as mechanical strength and toughness, high heat and chemical resistance and low moisture absorption [16]. The joining of composite structures using poly (vinylidene fluoride) (PVDF) was recently disclosed in a recent patent and the excellent compatibility between PVDF and

* Corresponding author. Institute of Technology Research and Innovation, Deakin University, Waurn Ponds, Victoria 3217, Australia. Tel.: +61 3 5227 1305.
E-mail address: kmagn@deakin.edu.au (K. Magniez).

0032-3861/$ – see front matter © 2010 Elsevier Ltd. All rights reserved.
doi:10.1016/j.polymer.2010.04.021

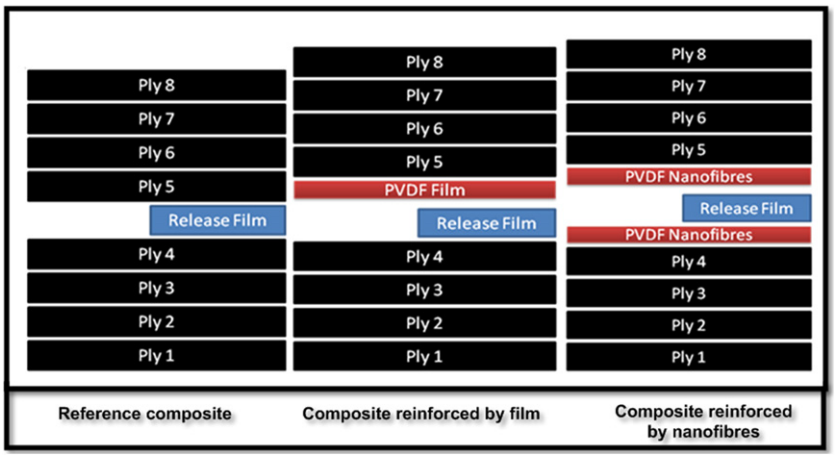

Fig. 1. Schematic of the staking sequence for the manufacture of the reference, film-modified and nanofibres-modified composite samples (note that the thickness of the release film, PVDF films and nanofibres are not to scale and appear thicker for visual clarity).

epoxy resin was also demonstrated [17]. For this reason, the interlaminar toughening of a carbon-fibre reinforced composite by incorporation of electrospun PVDF nanofibrous membranes was explored in this paper. The work aimed to determine the complex interfacial interactions between the nanofibres and the epoxy matrix, and understand how a secondary interlayer phase influences on the resistance to crack propagation in the resulting composites. The fracture toughness results were correlated to the micromechanisms of failure, changes in polymorphic crystal forms and molecular weights in order to establish the structure-property relationships. Finally, this article will discuss the effect of interlayer modification on the thermo-mechanical performance of the resulting composites and the changes in both properties and glass transitions will be interpreted.

2. Materials and experimental procedures

2.1. Materials

Carbon fibre reinforced composites were manufactured using Toray G83C (12 K 2 × 2 twill 380 gsm) supplied by Toray Composites Tacoma, Washington USA.

Polyvinylidene fluoride (PVDF) Kynar®710 and Kynar®740 were sourced from Arkema in the form of either pellets or films (50 μm thickness). Kynar®710 is a low molecular weight (LMW) PVDF having a number average molecular weight (M_n) in the range of 70,000–80,000 and Kynar®740 is a high molecular weight (HMW) PVDF having a number average molecular weight (M_n) 250, 000. Both grades melt at approximately 165 °C–170 °C and have a density of approximately 1.78 g/cm^3.

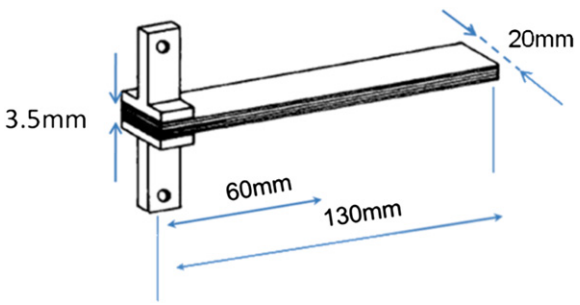

Fig. 2. Sample geometry for double cantilever beam (DCB) fracture toughness test.

2.2. Preparation of PVDF nanofibrous membranes by electrospinning

Polyvinylidene fluoride (PVDF) solutions at 10 wt.%, 15 wt.%, 20 wt.%, 25 wt.% and 30 wt.% concentrations were prepared by dissolving pellets in 8:2 volume ratios DMF/acetone solvent with stirring overnight at 70 °C. The solution were placed in a 5 ml medical syringe (0.8 mm needle diameter) connected with laboratory single jet system (KDS Syringe Pump) placed on a moving platform (velocity of 3 mm/s). The optimisation process was achieved by electrospinning PVDF nanofibrous membranes directly onto Toray G83C ply that was placed on a collector using voltages of 15 kV, 20 kV and 25 kV (Gamma power supply ES40P model).

The low and high molecular weights PVDF nanofibrous membranes used in the composites were produced by electrospinning directly onto the Toray G83C ply that was stuck using conductive carbon tape onto a cylinder rotating (120 rpm, 26 m/min), using voltages of 15 kV and 20 kV and solution concentrations of 30 wt.% and 25 wt.%, respectively. The flow rate and the needle tip-to-collector distance were set to 1.5 ml/h and 15 cm, respectively.

2.3. Composite manufacture

Five types of composites were produced for this work: a reference composite, two composites reinforced with approximately 5 wt.% in the laminates' mid-plane of low and high molecular weight PVDF nanofibrous membranes and two composites reinforced with a 50 μm film of the same low and high molecular weight PVDF (approximately accounting for 5 wt.%).

A symmetric lay-up sequence [0/90] was achieved by stacking 8 plies of pre-impregnated G83C woven fabric on top of each other,

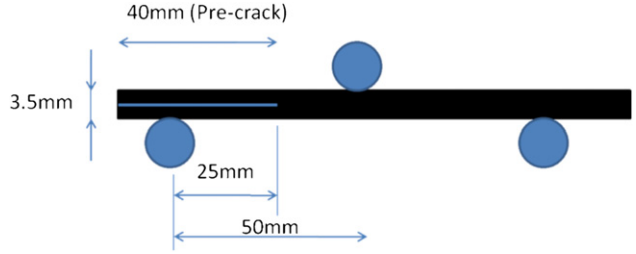

Fig. 3. Sample geometry for end notch flexure double (ENF) fracture toughness test.

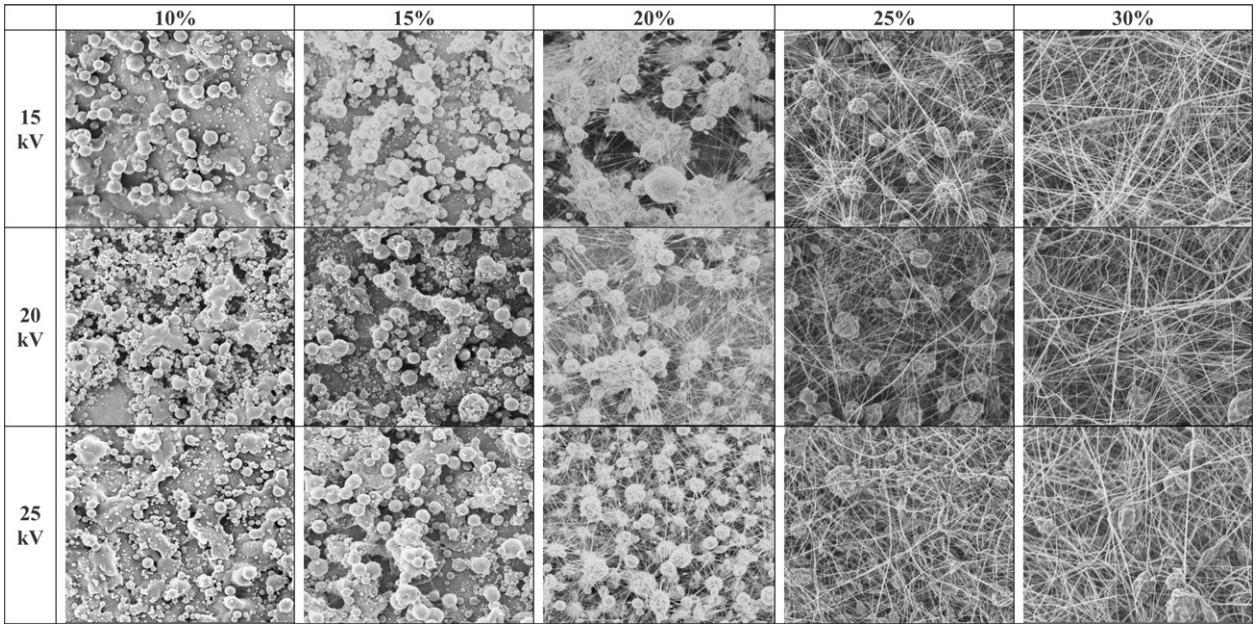

Fig. 4. Morphology of the LMW PVDF nanofibres (polymer flow rate 1.5 ml/min, tip to collector distance of 15 cm) showing the presence of beads and inhomogeneities. Nanofibres displaying minimum defects were obtained at (15 kV;30 wt.%).

which was then cured on an aluminium plate coated with a release agent. Since the fracture toughness was to be evaluated by allowing the crack to propagate only between the fourth and the fifth plies, the PVDF film was placed between those respective plies. The nanofibrous membranes however were deposited on both the fourth and the fifth plies (Fig. 1). A release film was inserted in one end of the laminates between the fourth and fifth plies as a pre-crack for the DCB and ENF tests. The thickness of all produced laminates was 3.5 mm $\pm$ 0.2 mm.

In order to remove any entrapped air between the layers during lay-up, de-bulking was performed every second ply for 10 min at room temperature. In addition, the plies containing the nanofibrous membranes were degassed for 2 h in a vacuum oven to remove any excess of solvent from the electrospinning process. The laminates were vacuum bagged at 70 kPa overnight prior to and during cure. G83C is a fast curing epoxy-based resin system designed to cure in 10 min at 150 °C. The curing cycle employed in this work was a ramp from room temperature to 150 °C at approximately 2 °C/min, followed by a dwell for 10 min before cooling.

2.4. Testing

2.4.1. Double cantilever beam (DCB) fracture toughness (mode I)

DCB testing was performed in the perpendicular direction to the length under a constant speed of 1 mm/min using 1 kN load using a Lloyd tensile testing machine following the protocol for

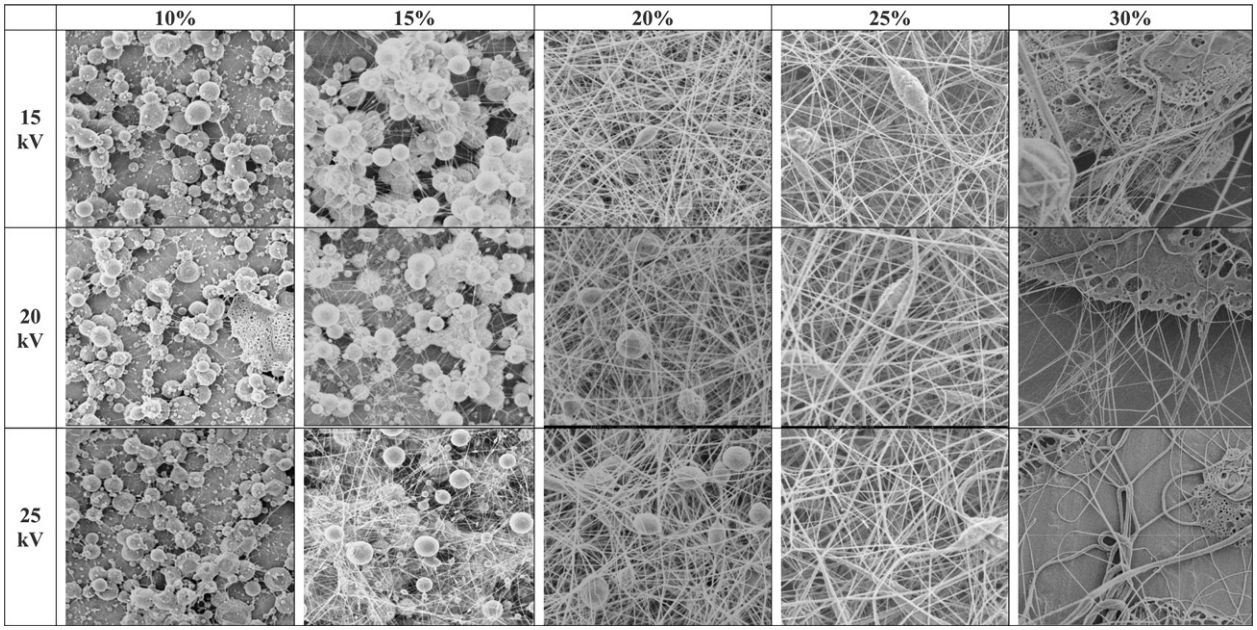

Fig. 5. Morphology of the HMW PVDF nanofibres (polymer flow rate 1.5 ml/min, tip to collector distance of 15 cm) showing the presence of beads and inhomogeneities. Nanofibres displaying minimum defects were obtained at (20 kV;25 wt.%).

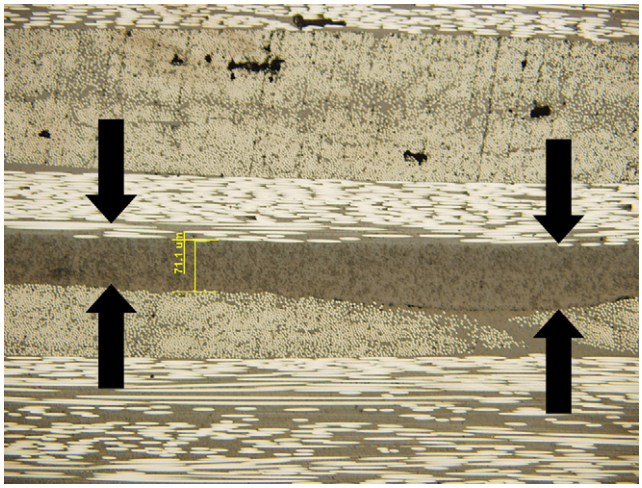

Fig. 6. Cross section optical images showing the interlayer electrospun membrane (highlighted between the arrows) between approximately 60 and 85 microns in thickness (only the LMW PVDF membrane is showed here for brevity).

interlaminar fracture testing (European Structural Integrity Society Standard) [18]. The dimensions of the DCB test samples were approximately 130 mm × 20 mm × 3.5 mm with a pre-crack length of 60 mm. Five DCB specimens were cut from the laminates using a diamond saw. Aluminium blocks were bonded onto the two sides of the specimen end having the pre-crack (Fig. 2). One side edge of the specimen was marked with white paint every 1 mm for the first 5 mm, and then, every 5 mm in order to facilitate the measurement of crack length. All samples were dried the day prior to testing (24 h, 70 °C). The width and the thickness of each specimen to the nearest 0.05 mm, at the midpoint and at 25 mm from both ends were measured, and their average values were calculated. The corrected beam theory described in the standard [18] was used to calculate G_{IC} values using the following equation:

Where P is applied load, δ is displacement, B is specimen width, a is crack length, and $|\Delta|$ is the crack length correction factor, which is found experimentally by plotting the cube root of compliance, $C^{1/3}$ as a function of a.

2.4.2. End notch flexure (ENF) fracture toughness

ENF testing was performed in a three-point bending mode (Fig. 3) using an Instron tensile testing machine with a crosshead speed of 1 mm/min following the protocol for interlaminar fracture testing (European Structural Integrity Society Standard) [19]. The dimensions of the ENF test samples were approximately 130 mm × 20 mm × 3.5 mm with a pre-crack length of 40 mm (Fig. 3). The width and thickness of each specimen was measured to the nearest 0.025 mm at the midpoint and at 10 mm from each end. Five ENF specimens cut from the laminates using a diamond saw were used for this test. The direct beam theory described in the standard was used to calculate G_{IIc} using the following expression [19]:

$$G_{IIc} = \frac{9a^2P\delta}{2B\left(2L^3 + 3a^3\right)}$$

Table 1
Fracture toughness (mode I) results.

	Critical Load (N)	G_{IC} (average) kJ/m^2	G_{IC} (max) kJ/m^2
Reference	44.1 ± 6.25	1.02 ± 0.1	1.26
LMW PVDF film	12.8 ± 3.85	0.1 ± 0.02	0.1
LMW PVDF nanofibres	45.7 ± 6.8	0.8 ± 0.07	0.9
HMW PVDF film	14.15 ± 2.75	0.2 ± 0.03	0.24
HMW PVDF nanofibres	46.78 ± 6.4	0.8 ± 0.14	1.09

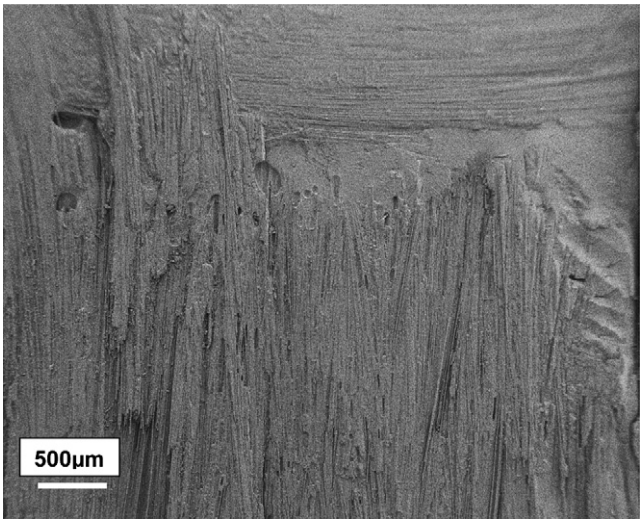

Fig. 7. SEM fractography images of the reference sample after DCB test.

where a is the crack length, P is the load, δ is the displacement, B is the specimen width and L is the half span.

2.4.3. Dynamic and mechanical analysis (DMTA)

Samples cut from the laminate of approximate dimensions of 60 mm (length) × 15 mm (width) × 3.5 mm (thickness) were used. Analysis was performed in a bending deformation mode using dual cantilever geometry using a frequency of 1 Hz. The experiments were carried out between 25 °C and 250 °C at a heating rate of 2 °C/min and a strain of 0.05%. The glass transition of the polymer blend was determined at maximum of loss tangent tan (δ) curve.

2.4.4. Differential scanning calorimetry (DSC)

The thermal analysis was performed on a TA Instruments Q200 differential scanning calorimeter. The instrument was operated under a nitrogen stream at a flow rate of 20 mL/min. Samples sealed in aluminium pans weighing approximately 10 mg were scanned by dynamically from room temperature up to 260 °C at 10 °C/min. The melting temperature T_m was defined as the endothermic peak maxima.

2.4.5. Fourier transform infrared spectroscopy (FTIR)

Infrared data were collected on a Bruker Vertex 70 FTIR equipped with an ATR unit. The spectra were obtained in attenuated total

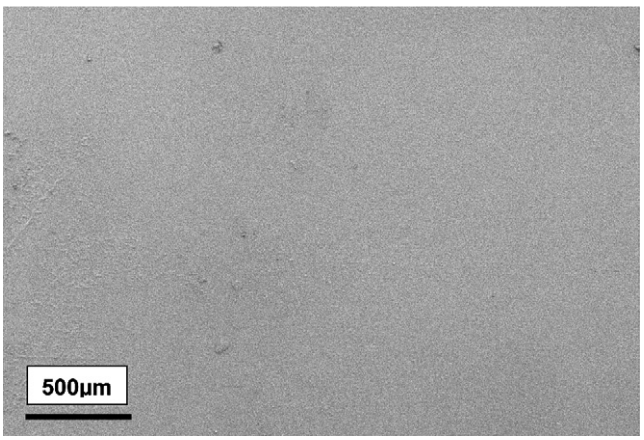

Fig. 8. SEM fractography images of LMW PVDF film modified composite samples showing a smooth surface morphology.

reflectance mode using section of electrospun PVDF membranes. 64 scans at 4 cm^{-1} resolution were collected for each sample between 600 cm^{-1} and 1600 cm^{-1}. The data were analysed using OPUS version 5.5 software.

2.4.6. Scanning electron microscopy (SEM)

The morphologies of nanofibrous membranes and the surface morphology of the composite samples after DCB fracture were observed using a scanning electron microscope (LEICA S440). The samples were vacuum coated with gold using a Balzers sputter coater. All images were taken using an accelerating voltage of 5–10 keV with a magnification between 200 times and 2000 times.

2.4.7. Optical microscopy

The thickness of the low and high molecular weight nanofibrous membrane was measured by imaging a cross section of each laminate. In order to understand the crack propagation mechanism during the DCB testing, a section was taken alongside the DCB samples at a crack length between 10 and 25 mm ± 5 mm.

Prior to imaging these samples were mounted in casting resin, ground and finely polished to a 1 μm surface finish using a RotoPol 21 polishing unit. Optical micrographs were taken using an Olympus DP70 digital camera at 5 and 10 times total magnification coupled with an Olympus BX51M optical microscope.

3. Results and discussion

3.1. Morphology of the PVDF nanofibrous membranes

The physical properties of the electrospun nanofibres such as fibre shape, diameter, surface morphology, or porosity are often strongly influenced by the electrospinning parameters [20]. This is well illustrated from the SEM images of the low and high molecular weights PVDF nanofibres taken at various solution concentration (10–30 wt.%) and various voltages (10–25 kV) (Figs. 4 and 5). The presence of beads and inhomogeneities is noticeable in the majority of the images. Nonetheless, using the optimum conditions of (15 kV, 30 wt.%) and (20 kV, 25 wt.%) for the low and high molecular weight PVDF respectively, nanofibres displaying minimum defects, orientation in random directions. Average nanofibre diameters of 213 nm ± 70 nm and 340 nm ± 150 nm were measured for the low and high molecular weight PVDF membranes, respectively.

Low and high molecular weights PVDF were electrospun directly onto the pre-impregnated woven material. Optical microscopy analysis of the cross section of the resulting composites revealed that the thickness of the interlayer membranes varied approximately between 60 and 85 microns (Fig. 6).

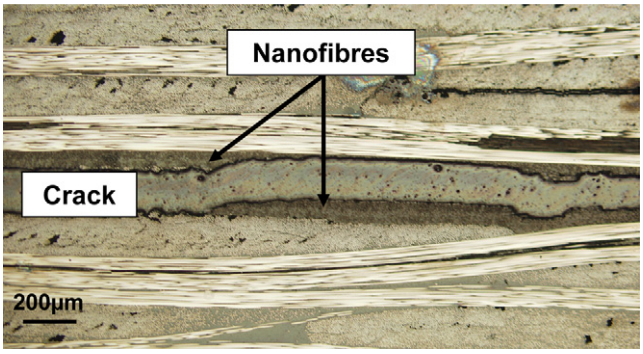

Fig. 9. Cross section optical images showing that the crack path transited from the mid-section of the nanofibrous interlayer region to the interfacial interlayer/resin region in the composites modified with PVDF nanofibres.

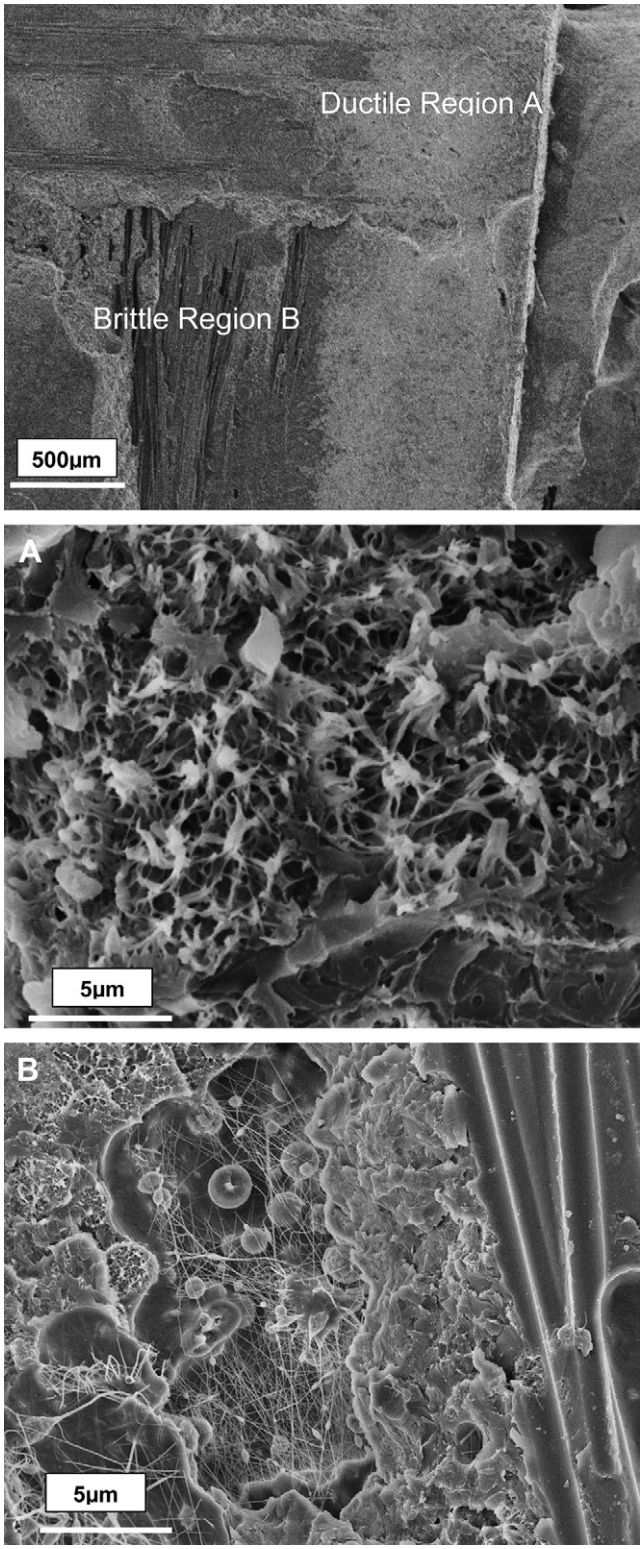

Fig. 10. Surface morphology of the composites modified with low molecular weight PVDF nanofibres showing a complex surface morphology after fracture (DCB) with a dominance of ductile regions and some brittle regions. Magnified images in the brittle region (B) showing PVDF nanofibres and microspheres whereas in the ductile region (A), plastically deformed nanofibres embedded into the matrix are visible.

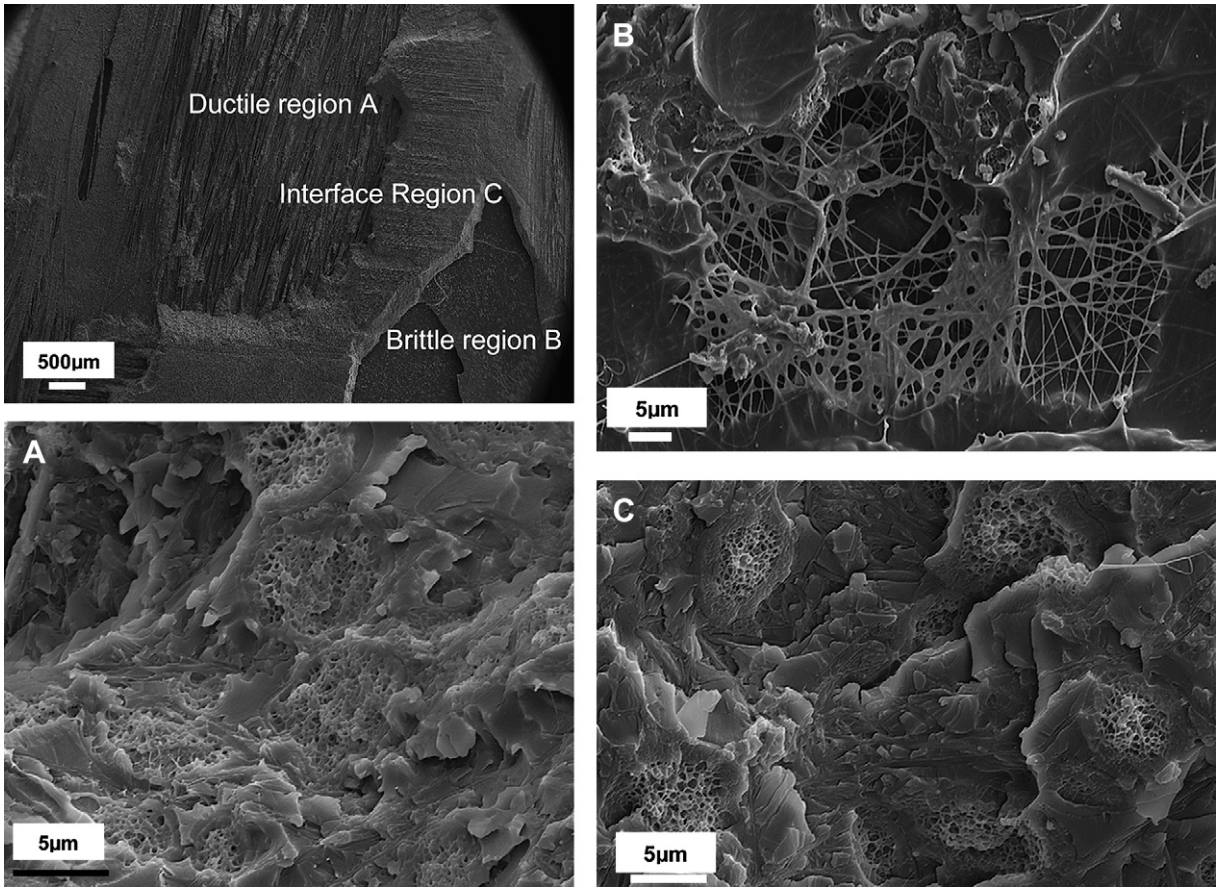

Fig. 11. Surface morphology of the composites modified with high molecular weight PVDF nanofibres showing a complex surface morphology after fracture (DCB) with the presence of mixed brittle and ductile regions. Magnified image (A) in the ductile region show plastically deformed elongated nanofibres well integrated within the epoxy matrix. Magnified image (B) in the brittle region show the presence of local nanofibres embedded within the epoxy matrix. Magnified image (C) in the interfacial region show porous bone-like structures.

3.2. Double cantilever beam (DCB) fracture toughness (mode I)

Evaluation of the fracture toughness in composite laminates is very important since the debonding between plies (referred to as interlaminar delamination) can significantly compromise the integrity of the structure. Interlaminar delamination often results from the formation and propagation of microcracks which are caused by thermal and mechanical stresses. The study of delamination in composites is often carried out by testing their fracture toughness in various modes of failure (namely opening, in-plane shear and anti-plane shear) [3]. The double cantilever beam (DCB) fracture toughness (mode I) represents the resistance of a material to delaminate in an opening mode of failure upon crack propagation (Fig. 2). The mode I fracture toughness (referred to as GIC) results are summarised in Table 1. It can be noted that the unmodified reference sample out-performed the other modified samples and displayed the best resistance to crack propagation with an average value GIC of 1.02 kJ/m^2. Surface fractography

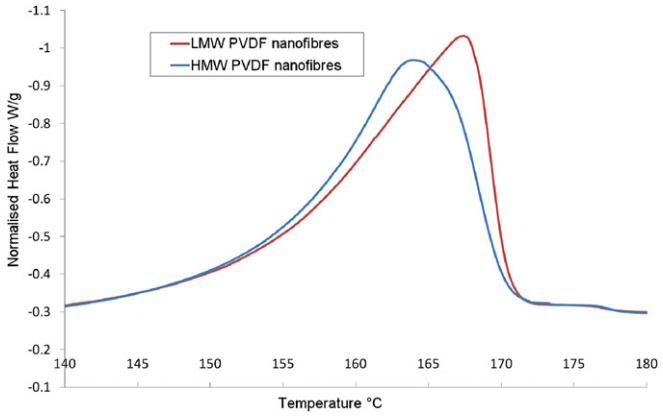

Fig. 12. DSC melting endotherms of the low molecular weight (LMW) and high molecular weight (HMW) PVDF nanofibrous membranes.

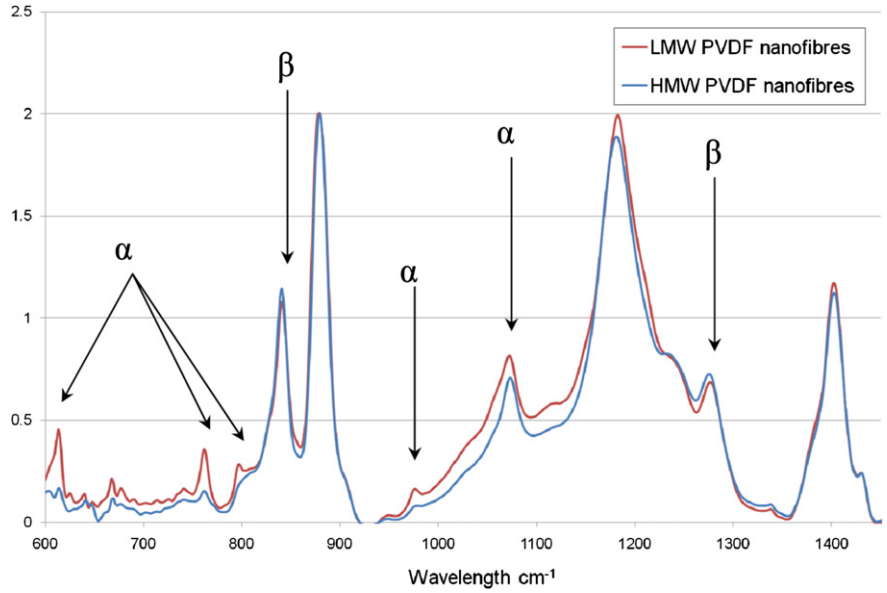

Fig. 13. FTIR-ATR spectra of the low molecular weight (LMW) and high molecular weight (HMW) PVDF nanofibrous membranes between 600 cm^{-1} and 1500 cm^{-1}. The α-phase is visible at 615 cm^{-1}, 760 cm^{-1}, 800 cm^{-1}, 980 cm^{-1} and 1075 cm^{-1}. The β-phase is visible at 840 cm^{-1} and 1276 cm^{-1}.

analysis revealed a typical brittle interlaminar fracture surfaces (Fig. 7) where interfacial debonding between the matrix and the carbon fibres appears to be the dominant failure mode.

The resistance to crack propagation for the samples containing the PVDF films were found to be very poor with average GIC values as low as 0.1 and 0.2 kJ/m^2, for the low and high molecular weight PVDF films, respectively. The surface topography of the samples was found to be smooth and a thin layer of PVDF was visible on both sides of the fractured DCB sample indicating that the film sheared off in its mid-plane (Fig. 8). Hence, it was concluded that adhesion properties between PVDF and the epoxy matrix were favourable but the shear strength properties of the films must have been too poor to provide any reinforcing effect. The GIC value for the samples modified with the high molecular weight film was higher than that of the low molecular weight film counterpart. This result was somehow expected as the shear strength properties of polymer used as bonding agents usually increases with increasing molecular weight [21].

The resistance to crack propagation for the samples containing the PVDF nanofibrous membranes were found to be slightly lower than the one of the reference sample with an average value GIC of 0.8 kJ/m^2 for both the low and high molecular weight samples (Table 1). This trend is somehow consistent with the recently reported literature showing no effect on the mode I results after incorporation of electrospun epoxy ultrathin fibres into a glass/epoxy composite [14]. Dzenis who pioneered this novel approach found a modest increase of 15% using polybenzimidazole (PBI) electrospun nanofibres (300–500 nm diameter range) in the interlayer of a unidirectional carbon fibre epoxy composite (Hexcel T2G190/F263) [11]. Others reported a more significant improvement by up to 280% using polysulfone nanofibres [12,13].

A cross section analysis of the DCB samples was analysed using optical microscopy in order to understand the mechanism of crack propagation. It was found that the crack path transited from the mid-section of the nanofibrous interlayer region to the interfacial interlayer/resin region (Fig. 9). This type of behaviour has previously been described in interlayer toughened systems and it was attributed to complex changes in micromechanisms of failure during the loading [5,22].

It is well documented that the mechanical properties of thermoplastic materials such as PVDF are directly correlated to their molecular weight [23]. Increases in mechanical performance are generally observed with increasing molecular weight of the polymer. More recently, it has also been shown that increasing the molecular weight of the thermoplastic in interlayer toughened composite systems will result in a further improvement in the resulting toughness of the system [24]. It is therefore sensible to say that the mode I fracture toughness of the composites modified with the nanofibrous membranes studied in this work should have been in principle reflecting the respective changes in molecular weights. Nonetheless and surprisingly, the composites containing either the low or the high molecular weight PVDF nanofibrous membranes showed similar fracture resistance behaviour with identical average GIC. The changes in the mode of interactions between the nanofibres and the epoxy matrix were believed to be responsible for this trend. This hypothesis was elucidated from the SEM images which illustrated very well the changes in the micromechanisms of failure (Figs. 10 and 11).

It can be noted that both samples modified with the nanofibrous membranes presented a surface topography showing a combination of brittle and ductile regions which evidenced the complexity of the micromechanisms of failure. Plastic deformation of the matrix and the nanofibres was visible (Figs. 10 and 11) in the semi-ductile regions and typical brittle interlaminar fracture surfaces accompanied with the presence of nanofibres embedded within the epoxy matrix were also visible. The high molecular weight sample exhibited some interesting porous bone-like structures surrounded by epoxy matrix (Fig. 11) in the interfacial regions possibly arising for partially wetted nanofibrous membrane. The surface of the composites modified with low molecular weight PVDF nanofibres showed a more ductile surface morphology (with

Table 2
Relative fraction F(β) of the β phase in the low and high molecular weight PVDF nanofibres.

Sample	A_α (615 cm^{-1})	A_α (766 cm^{-1})	A_β (840 cm^{-1})	F(β)[a]	F(β)[b]
LMW PVDF	0.4558	0.35833	1.05191	70	65
HMW PVDF	0.15781	0.14309	1.14351	87	85

[a] using the absorption bands at 766 cm^{-1} for the α phase.
[b] using the absorption bands at 615 cm^{-1} for the α phase.

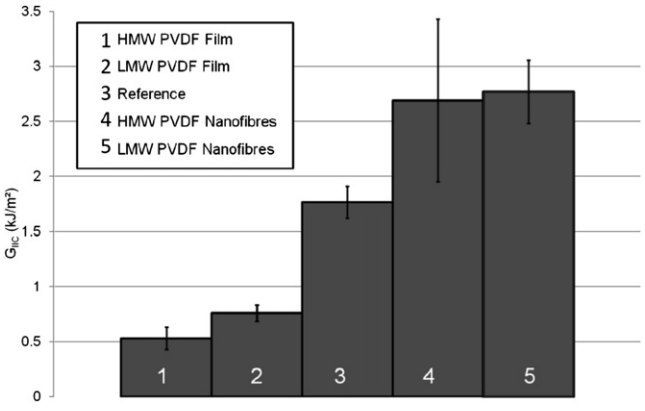

Fig. 14. End notch fracture test results (GIIC) for the reference composite and composite modified with low and high molecular weight (LMW and HMW, respectively) PVDF film and nanofibres.

the predominance of plastically deformed and elongated nanofibres) than the high molecular weight counterpart.

The difference in surface morphology and level of plastic deformation that has been observed between the two composites modified with nanofibrous membranes is believed to arise from the polymorphic nature of PVDF. Indeed, depending on the process conditions, PVDF can exhibit up to five different polymorphs, but generally the non-polar α phase to the polar β phases are the most common [25]. While the α phase is the most stable polymorph, the transition from the non-polar α phase to the polar β phase is often observed after thermal treatment or unidirectional stretching [26]. In more recent times, it has been reported that the electrospinning conditions have an influencing effect on the polymorphic behaviour of PVDF [25,27].

In this work, there were some elements in the DSC melting endotherms of the nanofibrous membranes (Fig. 12) suggesting that the polymorphic behaviour of PVDF varied between the various samples. The single melting endotherm at 167 °C displayed by the low molecular weight membrane was found to be a rather sharp transition. On the other hand, the single melting endotherm at 163.5 °C displayed by the high molecular weight membrane presented a shoulder at higher temperature, possibly emerging from the presence of a higher ratio of the β crystal phase. Previous work on the crystallisation of PVDF demonstrated that the melting behaviour is often complex [28,29], thermal history and molecular weight have been found to strongly affect on the localisation of the various polymorphs in the respective DSC melting thermographs [28,30]. The positions of the melting peaks have been attributed to the α, β and γ polymorphic phases from the lowest to the highest melting peak temperature, respectively. Our results correlate well with the ones reported by Gregorio et al. [31] who reported that the melting peaks of both the α and the β phase overlapped at approximately 167 °C.

The variation in polymorphic behaviour exhibited by the PVDF was also detected in the FTIR spectra (Fig. 13). In each sample, the appearance of absorption bands at 615 cm^{-1}, 765 cm^{-1}, 800 cm^{-1}, 980 cm^{-1} and 1075 cm^{-1} is an indication of α phase formation, however intensive absorption bands at 840 cm^{-1} and 1276 cm^{-1} are evidence of the high content of the β phase [25,26,31]. The fraction of β phase present in each sample can be calculated using the procedure explained by Gregorio [31] using an average total monomer concentration C of 0.0305 mol/cm^3, average crystalline densities of 1.925 g/cm^3 and 1.973 g/cm^3, absorption coefficients of 6.1×10^4 and 7.7×10^4 for the α and β phase respectively. The

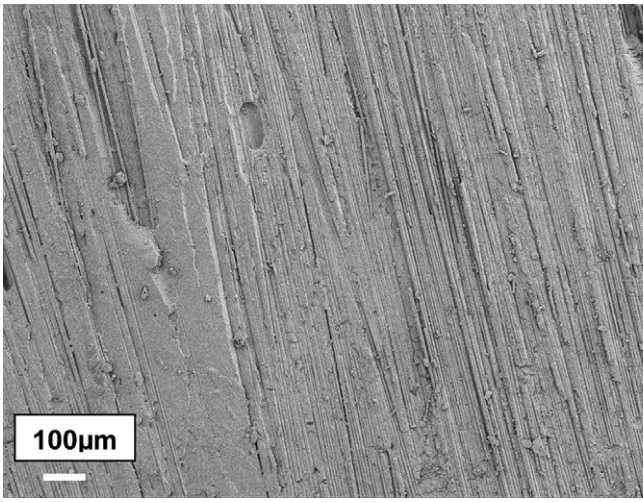

Fig. 15. Surface fractography of the reference composite after ENF testing. The presence of creases left after shear deformation is visible on the surface.

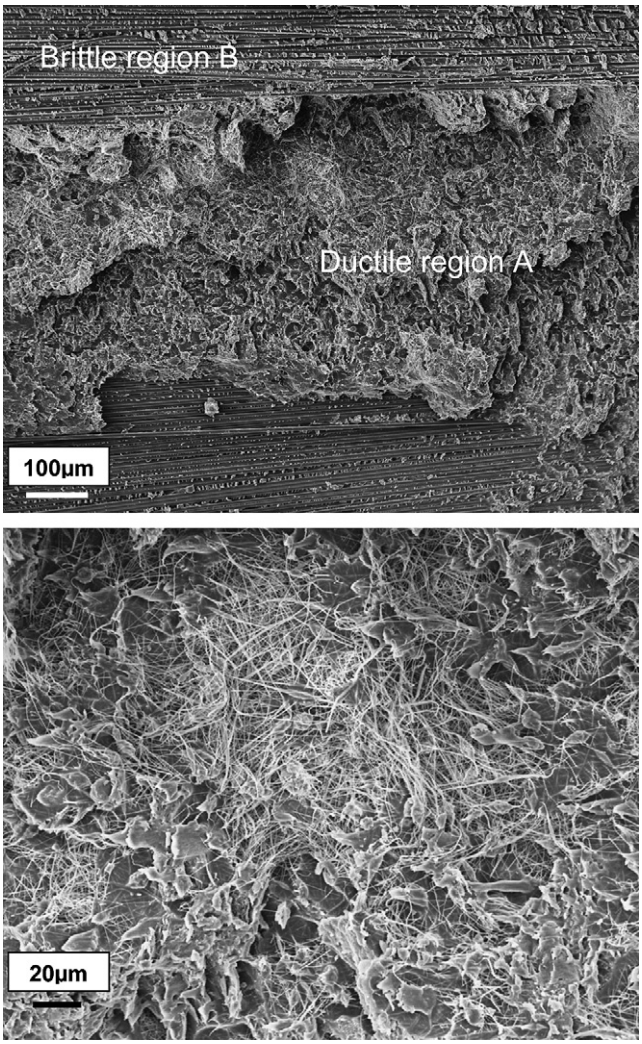

Fig. 16. Surface morphology of the composites modified with high molecular weight PVDF nanofibres showing a complex surface morphology after fracture (ENF) with the presence of mixed brittle and ductile regions. Magnified image in the ductile region (bottom image) shows deformed matrix (shear mode) and nanofibres.

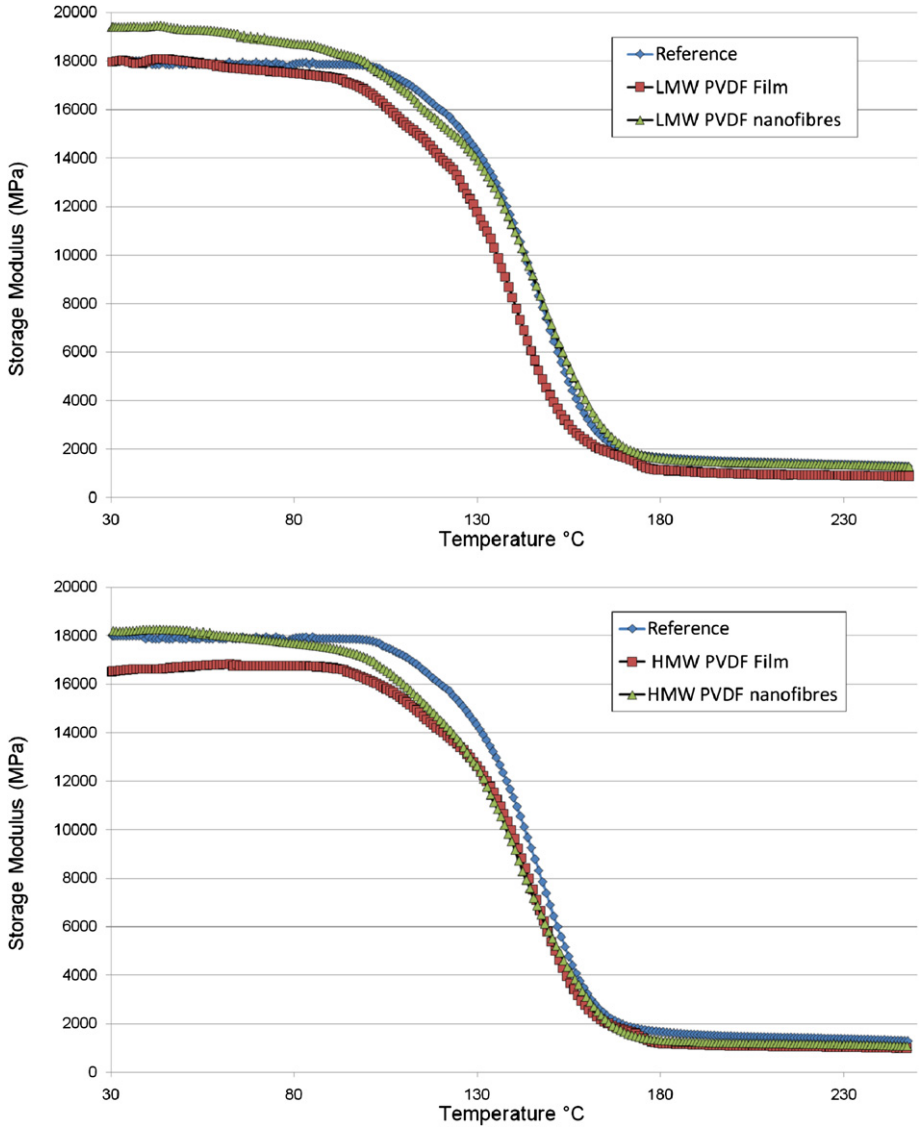

Fig. 17. Elastic response (E') of the reference composite and composites modified with low and high molecular weight (LMW and HMW, respectively) PVDF film and nanofibres Fig. 19. Loss tangent (tan δ) of the reference composite and composites modified with high molecular weight (HMW) PVDF film and nanofibres as such (top) and annealed (bottom).

relative fraction F(β) of the β phase can then be calculated using the following equation:

$$F(\beta) = \frac{\chi_\beta}{\chi_\alpha + \chi_\beta} = \frac{A_\alpha}{1.26A_\alpha + A_\beta}$$

where χ_α and χ_β are the degrees of crystallinity of each phases, and A_α and A_β correspond to absorption bands for α and β phases, respectively.

While the absorption band A_β at 840 cm^{-1} has typically been used to in the calculation of F(β), the position of the absorption band A_α has varied in the literature depending on the intensity of the signal. Gregorio [31] and Salimi [26] for instance used 766 cm^{-1} and 530 cm^{-1}, respectively. In this work, the absorption bands at both 615 cm^{-1} and 766 cm^{-1} were selected for the absorbance A_α of the α phase and 840 cm^{-1} for the β phase. From the F(β) values expressed in Table 2, it can be noted that the β phase accounts for approximately 65–70% of the total crystal ratio in the low molecular weight sample, whereas it reaches 85–87% in the high molecular counterpart. In light of these results, it is speculated that the polymorphic behaviour displayed by PVDF in the nanofibrous membranes strongly influenced the fracture toughness of the resulting composites and had a profound effect on the micromechanisms of failure. The effect of polymorphism on the mechanical properties of polymers has been widely reported [32–34] and our results are somehow consistent with the variations in mechanical behaviour in injection moulded and compressed PVDF samples observed [30,35]. It was found that the differences mainly appeared after yield in tension which was attributed to the crystal re-organisation into β crystal form. In injection moulded samples the formation of the less ductile β form after necking was also accompanied by an increase of the stress at failure.

3.3. End notch flexure (ENF) fracture toughness (G_{IIC})

During the fracture toughness of composites using an end-notched flexure test (ENF), the micromechanisms of fracture are controlled by the in-plane shear plastic deformation of the matrix [3,36]. The mode II fracture toughness (referred to as G_{IIC}) results are displayed in Fig. 14. Effective interlayer toughening of composites has previously been reported using thermoplastic and

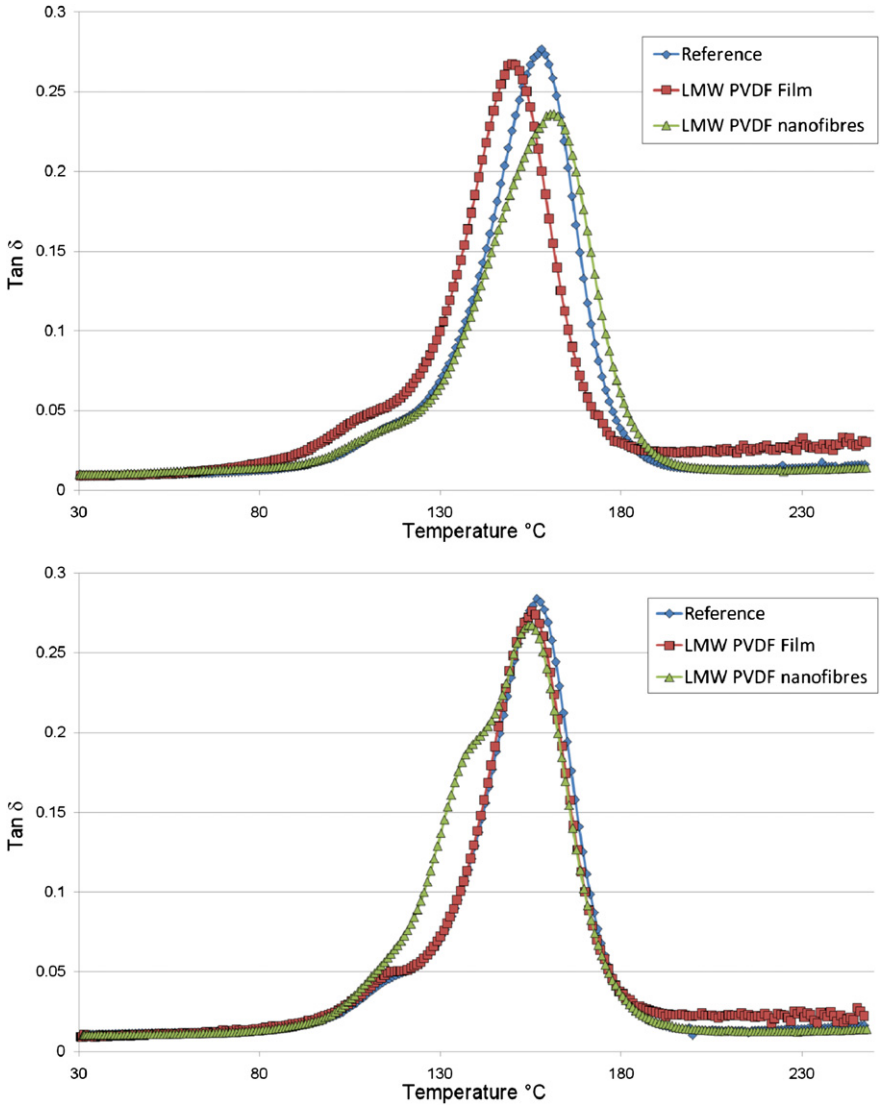

Fig. 18. Loss tangent (tan δ) of the reference composite and composites modified with low molecular weight (LMW) PVDF film and nanofibres as such (top) and annealed (bottom).

thermosets films [3,10,22,37–39]. The ability of the matrix to undergo plastic deformation has been correlated to the interlayer thickness and morphological features (shape, size and distribution) of the toughening phase. In this work, the surface morphology of the reference sample was found to be generally brittle and the shear plastic deformation of the matrix was noticeable from the presence of creases (Fig. 15). From the G_{IIC} results, it can be noted that the insertion of a PVDF film into the composite underperformed which highlights the inability for the epoxy matrix to plastically deform ahead of the crack tip. The surface morphology of the samples (not shown here for brevity) which were found to be very similar to the mode I images showed no sign of plastic deformation. The introduction of high and low molecular weights electrospun PVDF membranes on the other hand improved by approximately 53 and 57% respectively the G_{IIC} values of the resulting composites. The complex surface morphology after fracture (ENF) with the presence of mixed brittle and ductile regions was visible from the SEM images (Fig. 16). The ductility of the epoxy matrix in the presence of the nanofibres was also enhanced at the crack tip. The complexity in the crack path and micromechanisms of failure which have been aforementioned might have been in themselves contributing to the observed improvements. These results are in line with the ones published by Dzenis [11] who reported an increase of 130% in the mode II values. By using chopped Kevlar fibres grade 49 (12 μ in diameter) as an interlayer, Sohn et al. reported significant fibre bridging effects which resulted in increases of up to 100% in mode II.

3.4. Dynamic mechanical thermal analysis

Figs. 17–19 show the storage modulus (E′) and loss tangent (tan δ) of the samples between 30 °C and 250 °C, respectively. The thermo-mechanical properties of the composite samples were found to be relatively comparable over the range of tested temperatures (30–250 °C) and the addition of a PVDF interlayer did not result in any significant loss of the storage modulus. Nonetheless, the flexural modulus of 1.65 and 2.9 GPa [40] for the low and high molecular weight PVDF are much lower than that of the G83C carbon fibre composite (100 GPa [41]) and one might expect a more significant reduction in the storage modulus if an interlayer of PVDF was to be added between each plies of pre-pregs.

The Tg of the samples measured from the peaks of tan δ were found to be approximately 157°C ± 2 °C, except in the particular case of the sample modified with a low molecular weight PVDF film which

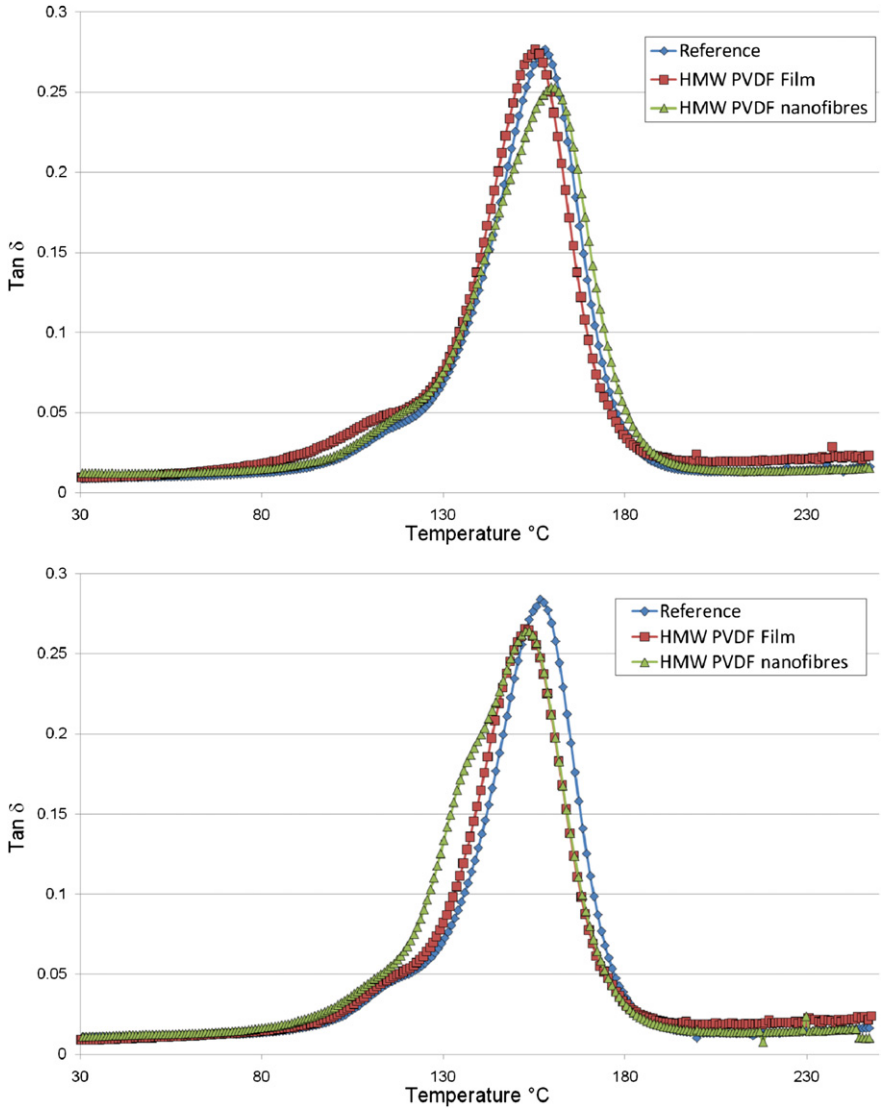

Fig. 19. Loss tangent (tan δ) of the reference composite and composites modified with high molecular weight (HMW) PVDF film and nanofibres as such (top) and annealed (bottom).

experienced a decrease of approximately 8 °C indicating a plasticising effect. Also of interest, the height of the tan δ peak for the samples modified with nanofibrous membranes slightly decreased possibly as a result of a stiffening of the network and a decrease of the amount of mobile chains near the glass transition region.

The presence of a shoulder at approximately 105 °C evidenced the presence of a phase separated PVDF in all composite samples (Figs. 18 and 19). Despite the occurrence of interfacial phase separation, there is strong evidence to suggest that a partial miscibility between the amorphous phases of the epoxy and PVDF exists. Annealing at 185 °C for 45 min resulted in a shift in Tg which implicates partial miscibility between the amorphous phases and high compatibility [42].

4. Conclusions

In this work, the electrospinning of a low and high molecular weight polyvinylidene fluoride (PVDF) was optimised through the control of the tip-to collector distance, voltage and flow rate parameters to form nanofibres free of defects with diameters averaging several hundreds of nanometres. The nanofibres were then directly deposited onto commercial pre-impregnated carbon fibre materials to produce a composite material. Under these conditions, PVDF primarily crystallised in its β phase polymorphic but higher contents of α form co-existed in the low molecular weight sample.

The interlaminar fracture toughness of composites modified with the nanofibrous membranes, and also thin films of the same low and high molecular weight PVDF, was measured by conducting double cantilever beam (mode I) and three-point bending (mode II). During these tests, the matrix is exposed at the crack tip to very different failure modes namely opening and in-plane shear deformation. An improvement of the plastic deformation of the epoxy after inclusion of the PVDF nanofibres was directly translated in a 57% increase in the mode II. On the other hand, a decrease of approximately 20% in the average G_{IC} values was observed which was attributed to the complexity in the micromechanisms of failure during mode I testing as evidenced from SEM fractography analysis. In addition, it is also speculated that the polymorphic behaviour displayed by PVDF had a profound effect on the fracture toughness of the resulting composites, and overpowered the anticipated effects of molecular weights which can explain the similarity in average G_{IC} values between the two high and low molecular weight samples. From these results, it is therefore suggested that a better

control over the polymorphic behaviour of PVDF and higher contents of the ductile α crystal phase during the electrospinning might probably improve the mode I fracture toughness of the resulting modified composites. It is also worth mentioning that although the adhesion properties between the PVDF film and the epoxy matrix were found to be favourable, the shear properties of the films also appeared to have been the limiting factor in their reinforcing and toughening effect.

Finally, the dynamic responses (i.e. storage modulus) of all composite samples were relatively found comparable over the range of tested temperatures. Nonetheless, after annealing above the melting point of PVDF, there is strong evidence to suggest that a partial miscibility between the amorphous phases of the PVDF nanofibres and the epoxy exists.

Acknowledgements

The authors thank Alfred Deakin Prof. Xungai Wang from the textile group at Deakin University for financial support of this research project. The authors gratefully acknowledge the helpful assistance of Associate Prof. Tong Lin and Dr. Jian Fang during this work and Glenn Bridgford from Arkema providing the Kynar® films.

References

[1] Available from, http://www.newairplane.com/787/design_highlights/; 2009.
[2] Hedrick JC, Patel NM, McGrath JE. Toughening of epoxy resin networks with functionalized engineering thermoplastics. In: Riew CK, Kinloch AJ, editors. Toughened plastics I, vol. 233. American Chemical Society; 1993. p. 293–304.
[3] Robinette EJ. PhD thesis: Toughening vinyl ester matrix composites by tailoring nanoscale and mesoscale interfaces, Chemical & Biological Engineering Department. Philadelphia: Drexel University; 2006.
[4] Yee AF. Modifying matrix materials for tougher composites. In: Johnston NJ, editor. ASTM STP 937 toughened composites. Philadelphia: American Society for Testing and Materials; 1987. p. 383–95.
[5] Hojo M, Matsuda S, Tanaka M, Ochiai S, Murakami A. Composites Science and Technology 2006;66:665–75.
[6] Nobuyuki O, Hajime K, Masaki Y. Advanced Composite Materials 1996;5(3):249–54.
[7] Hayes BS, Seferis JC. Journal of Composite Materials 2002;36:299–312.
[8] Sela N, Ishai O. Composites 1989;20(5):423–35.
[9] Yun N, Won Y, Kim S. Polymer Bulletin 2004;52(5):365–72.
[10] Min H, Kim S. Polymer Bulletin 1999;42:221–7.
[11] Dzenis Y, Reneker D. US Patent 626,333; 2001.
[12] Li G, Li P, Yu Y, Jia X, Zhang Z, Yang X, et al. Materials Letters 2008;62(3):511–4.
[13] Li G, Li P, Zhang C, Yu Y, Liu H, Zhang S, et al. Composites Science and Technology 2008;68(3–4):987–94.
[14] Liu L, Liang YM, Xu GI, Zhang HS, Huang ZM. Journal of Reinforced Plastics and Composites 2008;27:1–15.
[15] Sihn S, Kim RY, Huh W, Lee KH, Roy AK. Composites Science and Technology 2008;68:673–83.
[16] Available from, http://www.texloc.com/closet/cl_pvdf_properties.htm; 2009.
[17] Beehag A, Horton K, Cartwright B.US Patent EP20060291496; 2006.
[18] Protocol No 1 for interlaminar fracture toughness testing of composites: mode I. European Structural Integrity Society; 1993.
[19] Protocol No 2 for interlaminar fracture toughness testing of composites: mode II. European Structural Integrity Society; 1993.
[20] Huang Z-M, Zhang Y-Z, Kotaki M, Ramakrishna S. Composites Science and Technology 2003;63(15):2223–53.
[21] Cano RJ, Jensen BJ. The Journal of Adhesion 1997;60:113–23.
[22] Singh S, Partridge IK. Composites Science and Technology 1995;55(4):319–27.
[23] Nunes RW, Martin JR, Johnson JF. Polymer Engineering and Science 1982;22(4):205–28.
[24] Hodgkin JH, Simon GP, Varley RJ. Polymers for Advanced Technologies 1996;9:3–10.
[25] Zheng J, He A, Li J, Han C. Macromolecular Rapid Communications 2007;28:2159–62.
[26] Salimi A, Yousefi AA. Polymer Testing 2003;22:699–704.
[27] Yee WA, Kotaki M, Liu Y, Lu X. Polymer 2007;48:512–21.
[28] Sajkiewicz P. European Polymer Journal 1999;35:1581–90.
[29] Sajkiewic P, Wasiak A, Gocłowski Z. European Polymer Journal 1999;35(3):423–9.
[30] Mohajir B-EE, Heymans N. Polymer 2001;42(13):5661–7.
[31] Gregorio R, Cestari M. Journal of Polymer Science Part B: Polymer Physics 1994;32:859–70.
[32] Xie S, Zhang S, Liu H, Chen G, Feng M, Qin H, et al. Polymer 2005;46(14):5417–27.
[33] Fornes TD, Paul DR. Polymer 2003;44:3945–61.
[34] Tjong SC. Materials Science and Engineering: R: Reports 2006;53(3–4):73–197.
[35] Mohajir B-EE, Heymans N. Polymer 2001;42(16):7017–23.
[36] Todo M, Jar P-YB, Takahashi K. Composites Science and Technology 2000;60:263–72.
[37] Fracasso R, Rink M, Pavan A, Frassine R. Composites Science and Technology 2001;61:57–63.
[38] Evans RE, Hirschbuehler KR. Thermoplastic interleafed resin matrix composites with improved impact strength and toughness. US Patent 4604319; 1984.
[39] Naffakh M, Dumon M, Gerard JF. Composites Science and Technology 2006;66:1376–84.
[40] Available from, http://www.arkema-inc.com/kynar/page.cfm?pag=979; 2008.
[41] Available from, http://www.stateone.com.au/downloads/QHL%20Report.pdf; 2007.
[42] Simon GP. Polymer characterization techniques and their application to blends. American Chemical Society; 2003.